$V_2O_5 \cdot nH_2O$ Crystalline Nanosheets: Hydrothermal Fabrication and Structure Evolution

Xiao Kai Hu, De Kun Ma, Jian Bo Liang, Sheng Lin Xiong, Jiang Ying Li, and Yi Tai Qian*
Division of Nanomaterials and Nanochemistry, Hefei National Laboratory for Physical Sciences at Microscale, and Department of Chemistry, University of Science and Technology of China, Hefei, Anhui 230026, P. R. China

(Received January 24, 2007; CL-070084; E-mail: ytqian@ustc.edu.cn)

$V_2O_5 \cdot nH_2O$ nanosheets are fabricated hydrothermally with the acidified peroxovanadate solution at 200 °C for 12 h. The X-ray diffraction suggests that $V_2O_5 \cdot nH_2O$ nanosheets display lamellar ordering along *c*-axis direction. Transmission electron microscopy, field-emission scanning electron microscopy, and selected area electron diffraction indicate that $V_2O_5 \cdot nH_2O$ nanosheets are very thin in thickness and micron-sized in lateral dimension, and they are two-dimensional crystallites. X-ray photoelectron spectroscopy and thermogravimetric analysis are utilized to confirm the elemental composition of nanosheets. The formation process of nanosheets is also discussed in terms of time- and temperature-controlled experiments.

Hydrated vanadium pentoxide (or $V_2O_5 \cdot nH_2O$ xerogel) have been known for more than a century and studied extensively for their electrical, ionic, and electrochemical properties.[1–3] $V_2O_5 \cdot nH_2O$ displays lamellar ordering whereas the structure within the basal plane remains unclear.[4] Several methods have been established to fabricate $V_2O_5 \cdot nH_2O$, such as acidification and polymerization of (meta)vanadate,[5,6] hydrolysis and condensation of vanadium alkoxide,[7–9] reaction between V_2O_5 and H_2O_2,[10,11] and directly pouring the molten V_2O_5 into water.[4] In most cases, as-fabricated products are $V_2O_5 \cdot nH_2O$ nanobelts.

In this letter, we performed a hydrothermal treatment on the acidified peroxovanadate solution that was obtained by reacting V_2O_5 and H_2O_2. The resulting products are $V_2O_5 \cdot nH_2O$ nanosheets instead of traditionally observed $V_2O_5 \cdot nH_2O$ nanobelts. The controlled experiments further show that as-fabricated $V_2O_5 \cdot nH_2O$ nanosheets are the intermediate products between $V_2O_5 \cdot nH_2O$ nanobelts and crystalline V_2O_5 nanowires (For detailed experimental procedure, see Supporting Information[18]).

Figure 1 demonstrates the reflection X-ray diffraction (XRD) pattern of $V_2O_5 \cdot nH_2O$ nanosheets. The pattern displays only 00*l* reflections, implying that the V_2O_5 slabs and water layers may be assembled in an alternant way and nanosheets stack along *c* direction. The basal plane distance is determined to be 14.2 Å, according to the 00*l* peak positions, much larger than the basal spacing (4.37 Å) of orthorhombic V_2O_5 (JCPDS 77-2418).[12] The presence of 002 reflection in our XRD pattern, which is commonly absent in the literature, may hint some differences in structure between $V_2O_5 \cdot nH_2O$ nanosheets and previous $V_2O_5 \cdot nH_2O$.[3,4,6,10]

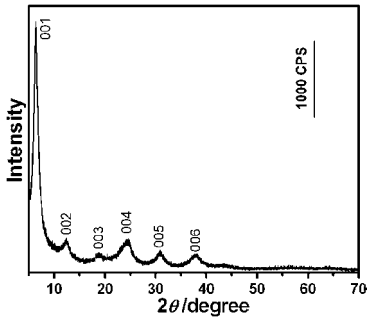

Figure 1. The reflection XRD pattern of $V_2O_5 \cdot nH_2O$ nanosheets.

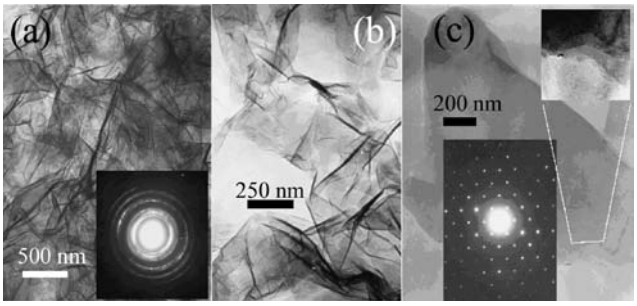

Figure 2. The low (a) and high (b) magnified TEM images of $V_2O_5 \cdot nH_2O$ nanosheets fabricated at 200 °C for 12 h; inset of (a) is the SAED pattern recorded on many nanosheets. (c) is the TEM image of a single nanosheet, with its SAED pattern (bottom inset) and a closer view (top right inset).

Figure 2 are the transmission electron microscopy (TEM) images of as-prepared $V_2O_5 \cdot nH_2O$ nanosheets. It is obvious that all the nanosheets have an ultrathin thickness, as evidenced by their faint contrast and folded morphology. As can be seen, the nanosheets are several microns in lateral size and irregular with respect to their brims. The inset in Figure 2a is a selected area electron diffraction (SAED) pattern recorded on many nanosheets. Figure 2c is a single $V_2O_5 \cdot nH_2O$ nanosheet and its SAED pattern (bottom inset), which exhibits the monocrystalline nature of two-dimensional (2D) $V_2O_5 \cdot nH_2O$ nanosheet. Closer view revealed that the nanosheet is made up of several monolayers (top right inset in Figure 2c). The 2D single-crystal nanosheet may be useful for understanding the in-plane structure of $V_2O_5 \cdot nH_2O$.[1,4] The field emission scanning electron microscopy (FESEM) image (Figure S1) further supports the ultrathin character of nanosheets.[18]

The X-ray photoelectron spectroscopy (XPS) spectrum of $V_2O_5 \cdot nH_2O$ nanosheets is depicted in Figure 3a. The peaks at 517.5 and 525.1 eV correspond to the binding energy of $V2p_{3/2}$ and $V2p_{1/2}$ electron of V^{5+}, respectively.[13] The peak at 530.35 eV represents the 1s electron binding energy of oxygen atom that is bonded with vanadium atom.[13] The binding energy of O1s electron associated with interlayer H_2O is 533.15 eV.[14] The thermogravimetric analysis (TGA) on $V_2O_5 \cdot nH_2O$ nanosheets is outlined in Figure 3b. The weight loss seems to undergo

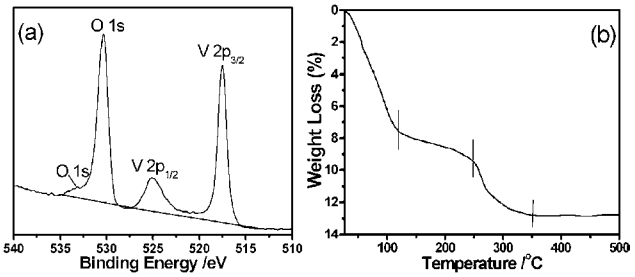

Figure 3. (a) The XPS spectrum of V2p and O1s electron in $V_2O_5 \cdot nH_2O$ nanosheets; (b) TGA curve of $V_2O_5 \cdot nH_2O$ nanosheets measured in air with heating rate of 5 °C per minute.

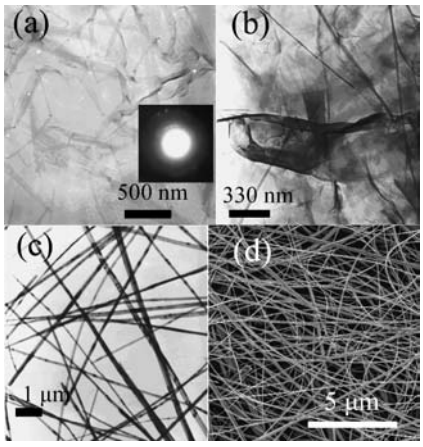

Figure 4. The TEM images of products prepared at 100 °C for 12 h (a) and 200 °C for 60 h (b); the TEM (c) and FESEM (d) image of V_2O_5 nanowires prepared at 220 °C for 48 h. Inset of (a) is a SAED pattern of $V_2O_5 \cdot nH_2O$ nanobelts.

three stages, being analogous to the literature data on $V_2O_5 \cdot nH_2O$ xerogel.[12] The first stage is due to the loss of absorbed and weak intercalated water; the second stage may represent the gradual release of strong bonded interlayer water; and the third stage corresponds to the abrupt exclusion of the interlayer water, during which the V_2O_5 slabs condense together, and V_2O_5 three-dimensional network forms as a result of structural rearrangements. The residual sample after TG analysis is V_2O_5 by XRD detection (Figure S2).[18] The corresponding XRD investigations also support the above analysis (Figure S3).[18] The n value in $V_2O_5 \cdot nH_2O$ nanosheets is calculated to be 1.5, according to the total weight loss.

In order to explore the formation process of $V_2O_5 \cdot nH_2O$ nanosheets, a series of controlled experiments are carried out. All the products are analyzed by XRD, and some results are shown in Figure S4.[18] Figure 4a is the TEM image of the products prepared hydrothermally at 100 °C for 12 h, which are $V_2O_5 \cdot nH_2O$ nanobelts. The SAED pattern (inset) shows $V_2O_5 \cdot nH_2O$ nanobelts are poor in crystallinity. The products available at 200 °C for 2 h are also $V_2O_5 \cdot nH_2O$ nanobelts. Figure 4b is the TEM image of the products obtained at 200 °C for 60 h, which are a mixture of $V_2O_5 \cdot nH_2O$ nanosheets and V_2O_5 nanowires. The products obtained at 220 °C for 12 h are the same mixture as those at 200 °C for 60 h. Figures 4c and 4d are TEM and FESEM images of the products prepared at 220 °C for 48 h, which are V_2O_5 nanowires.[15] All the results indicate that, during the hydrothermal process, $V_2O_5 \cdot nH_2O$ nanobelts are initially formed, and they tend to develop towards $V_2O_5 \cdot nH_2O$ nanosheets, which transform to V_2O_5 nanowires by dehydration. Obviously, the temperature and duration time of hydrothermal treatment are two crucial factors for these changes. The change process from nanobelts to nanosheets is rarely reported and its driving force is still unknown to us, but similar transformation from nanosheets to nanowires has been observed in preparation of MnO_2 and $V_2O_4 \cdot 0.25H_2O$ nanowires.[16,17]

The hydrochloric acid is vital to succeed in preparing $V_2O_5 \cdot nH_2O$ nanosheets; otherwise, the products are less in amount and often the mixture of $V_2O_5 \cdot nH_2O$ nanosheets or nanobelts and V_2O_5 nanowires. The $V_2O_5 \cdot nH_2O$ nanosheets are grown by polymerization reaction of the acidified peroxovanadate species in precursor solution.[11]

In conclusion, $V_2O_5 \cdot nH_2O$ nanosheets are fabricated in a hydrothermal way using V_2O_5, H_2O_2, and HCl as the starting reagents. The $V_2O_5 \cdot nH_2O$ nanosheets are two-dimensional crystals, and they are probably useful for understanding the structure of $V_2O_5 \cdot nH_2O$. $V_2O_5 \cdot nH_2O$ nanosheets are the intermediate products between $V_2O_5 \cdot nH_2O$ nanobelts and V_2O_5 nanowires. As-fabricated $V_2O_5 \cdot nH_2O$ nanosheets can be applied in preparation of high-quality vanadium pentoxide film by the layer-by-layer deposition.

This work is financially supported by the 973 project of china (No. 2005CB623601).

References and Notes

1 J. Livage, *Chem. Mater.* **1991**, *3*, 578.
2 B. Vigolo, C. Zakri, F. Nallet, J. Livage, C. Coulon, *Langmuir* **2002**, *18*, 9121.
3 O. Durupthy, N. Steunou, T. Coradin, J. Livage, *J. Mater. Chem.* **2005**, *15*, 1090.
4 V. Petkov, P. N. Trikalitis, E. S. Bozin, S. J. L. Billinge, T. Vogt, M. G. Kanatzidis, *J. Am. Chem. Soc.* **2002**, *124*, 10157.
5 J. Muster, G. T. Kim, V. Krstic, J. G. Park, M. Burghard, *Adv. Mater.* **2000**, *12*, 420.
6 J. F. Liu, X. Wang, Q. Peng, Y. D. Li, *Adv. Mater.* **2005**, *17*, 764.
7 F. Chaput, B. Dunn, P. Fuqua, K. Salloux, *J. Non-Cryst. Solids* **1995**, *188*, 11.
8 H. P. Wong, B. C. Dave, F. Leroux, J. Harreld, B. Dunn, L. F. Nazar, *J. Mater. Chem.* **1998**, *8*, 1019.
9 S. D. Desai, E. L. Cussler, *Langmuir* **1998**, *14*, 277.
10 Y. Wang, H. M. Shang, T. Chou, G. Z. Cao, *J. Phys. Chem. B* **2005**, *109*, 11361.
11 C. J. Fontenot, J. W. Wiench, M. Pruski, G. L. Schrader, *J. Phys. Chem. B* **2001**, *105*, 10496.
12 C. J. Fontenot, J. W. Wiench, G. L. Schrader, M. Pruski, *J. Am. Chem. Soc.* **2002**, *124*, 8435.
13 C. D. Wagner, W. M. Riggs, L. E. Davis, J. F. Moulder, G. E. Muilenberg, *Handbook of X-ray Photoelectron Spectroscopy*, Perkin-Elmer Corporation, **1978**.
14 K. Chiba, R. Ohmori, H. Tanigawa, S. Tanaka, *Fusion Engineering and Design* **2000**, *49–50*, 791.
15 G. C. Li, S. P. Pang, L. Jiang, Z. Y. Guo, Z. K. Zhang, *J. Phys. Chem. B* **2006**, *110*, 9383.
16 X. Wang, Y. D. Li, *Chem.—Eur. J.* **2003**, *9*, 300.
17 M. Wei, H. Sugihara, I. Honma, M. Ichihara, H. Zhou, *Adv. Mater.* **2005**, *17*, 2964.
18 Supporting Information is available electronically on the CSJ-Journal Web site, http://www.csj.jp/journals/chem-lett/index.html.

Published on the web (Advance View) March 27, 2007; doi:10.1246/cl.2007.560